Operational Amplifiers and Active Filters:
A Bond Graph Approach

Gilberto González and Roberto Tapia
University of Michoacan
Mexico

1. Introduction

The most important single linear integrated circuit is the operational amplifier. Operational amplifiers (op-amp) are available as inexpensive circuit modules, and they are capable of performing a wide variety of linear and nonlinear signal processing functions (Stanley, 1994).

In simple cases, where the interest is the configuration gain, the ideal op-amp in linear circuits, is used. However, the frequency response and transient response of operational amplifiers using a dynamic model can be obtained.

The bond graph methodology is a way to get an op-amp model with important parameters to know the performance. A bond graph is an abstract representation of a system where a collection of components interact with each other through energy ports and are place in the system where energy is exchanged (Karnopp & Rosenberg, 1975).

Bond graph modelling is largely employed nowadays, and new techniques for structural analysis, model reduction as well as a certain number of software packages using bond graph have been developed.

In (Gawthrop & Lorcan, 1996) an ideal operational amplifier model using the bond graph technique has been given. This model only considers the open loop voltage gain and show an application of active bonds.

In (Gawthrop & Palmer, 2003), the `virtual earth' concept has a natural bicausal bond graph interpretation, leading to simplified and intuitive models of systems containing active analogue electronic circuits. However, this approach does not take account the type of the op-amp to consider their internal parameters.

In this work, a bond graph model of an op-amp to obtain the time and frequency responses is proposed. The input and output resistances, the open loop voltage gain, the slew rate and the supply voltages of the operational amplifier are the internal parameters of the proposed bond graph model.

In the develop of this work, the Bond Graph model in an Integral causality assignment (BGI) to determine the properties of the state variables of a system is used (Wellstead, 1979; Sueur & Dauphin-Tanguy, 1991). Also, the symbolic determination of the steady state of the variables of a system based on the Bond Graph model in a Derivative causality assignment (BGD) is applied (Gonzalez et al., 2005). Finally, the simulations of the systems represented

by bond graph models using the software 20-Sim by Controllab Products are realized (Controllab Products, 2007).

Therefore, the main result of this work is to present a bond graph model of an op-amp considering the internal parameters of a type of linear integrated circuit and external elements connected to the op-amp, for example, the feedback circuit and the load.

The outline of the paper is as follows. Section 2 and 3 summarizes the background of bond graph modelling with an integral and derivative causality assignment. Section 4 the bond graph model of an operational amplifier is proposed. Also, the frequency responses of the some linear integrated circuits that represent operational amplifier using the proposed bond graph model are obtained. Section 5 gives a comparator circuit using a bond graph model and obtaining the time response. Section 6 presents the proposed bond graph model of an feedback op-amp; the input and output resistances, bandwidth, slew rate and supply voltages of a non-inverting amplifier using BGI and BGD are determined. Section 7 gives the filters using a bond graph model of an op-amp. In this section, we apply the filters for a complex signal in the physical domain. The bond graph model of an op-amp to design a Proportional and Integral (PI) controller and to control the velocity of a DC motor in a closed loop system is applied in section 8. Finally, the conclusions are given in section 9.

2. Bond graph model

Consider the following scheme of a Bond Graph model with an Integral causality assignment (BGI) for a multiport Linear Time Invariant (LTI) system which includes the key vectors of Fig. 1 (Wellstead, 1979; Sueur & Dauphin-Tanguy, 1991).
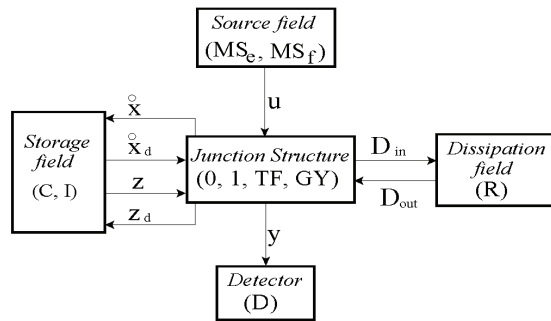

Fig. 1. Key vectors of a bond graph.

In fig. 1, $\left(MS_{e}, MS_{f}\right)$, $\left(C, I\right)$ and $\left(R\right)$ denote the source, the energy storage and the energy dissipation fields, $\left(D\right)$ the detector and $\left(0, 1, TF, GY\right)$ the junction structure with transformers, TF, and gyrators, GY.

The state $x(t) \in \Re^{n}$ and $x_{d}(t) \in \Re^{m}$ are composed of energy variables $p(t)$ and $q(t)$ associated with I and C elements in integral causality and derivative causality, respectively, $u(t) \in \Re^{p}$ denotes the plant input, $y(t) \in \Re^{q}$ the plant output, $z(t) \in \Re^{n}$ the co-energy vector, $z_{d}(t) \in \Re^{m}$ the derivative co-energy and $D_{in}(t) \in \Re^{r}$ and $D_{out}(t) \in \Re^{r}$ are a mixture

of $e(t)$ and $f(t)$ showing the energy exchanges between the dissipation field and the junction structure (Wellstead, 1979; Sueur & Dauphin-Tanguy, 1991).
The relations of the storage and dissipation fields are,

$$z(t) = Fx(t) \tag{1}$$

$$z_d(t) = F_d x_d(t) \tag{2}$$

$$D_{out}(t) = LD_{in}(t) \tag{3}$$

The relations of the junction structure are,

$$\begin{bmatrix} \dot{x}(t) \\ D_{in}(t) \\ y(t) \end{bmatrix} = \begin{bmatrix} S_{11} & S_{12} & S_{13} & S_{14} \\ S_{21} & S_{22} & S_{23} & 0 \\ S_{31} & S_{32} & S_{33} & 0 \end{bmatrix} \begin{bmatrix} x(t) \\ D_{out}(t) \\ u(t) \\ \dot{x}_d(t) \end{bmatrix} \tag{4}$$

$$z_d(t) = -S_{14}^T z(t) \tag{5}$$

The entries of S take values inside the set $\{0, \pm 1, \pm m, \pm n\}$ where m and n are transformer and gyrator modules; S_{11} and S_{22} are square skew-symmetric matrices and S_{12} and S_{21} are matrices each other negative transpose. The state equation is (Wellstead, 1979; Sueur & Dauphin-Tanguy, 1991),

$$\dot{x}(t) = A_p x(t) + B_p u(t) \tag{6}$$

$$y(t) = C_p x(t) + D_p u(t) \tag{7}$$

where

$$A_p = E^{-1}\left(S_{11} + S_{12}MS_{21}\right)F \tag{8}$$

$$B_p = E^{-1}\left(S_{13} + S_{12}MS_{23}\right) \tag{9}$$

$$C_p = \left(S_{31} + S_{32}MS_{21}\right)F \tag{10}$$

$$D_p = S_{33} + S_{32}MS_{23} \tag{11}$$

being

$$E = I_n + S_{14}F_d^{-1}S_{14}^T F \tag{12}$$

$$M = \left(I_n - LS_{22} \right)^{-1} L \tag{13}$$

3. Bond graph in derivative causality assignment

We can use the Bond Graph in Derivative causality assignment (BGD) to solve directly the problem to get A_p^{-1}. Suppose that A_p is invertible and a derivative causality assignment is performed on the bond graph model (Gonzalez et al., 2005). From (4) the junction structure is given by,

$$\begin{bmatrix} z(t) \\ D_{ind}(t) \\ y_d(t) \end{bmatrix} = \begin{bmatrix} J_{11} & J_{12} & J_{13} \\ J_{21} & J_{22} & J_{23} \\ J_{31} & J_{32} & J_{33} \end{bmatrix} \begin{bmatrix} \dot{x}(t) \\ D_{outd}(t) \\ u(t) \end{bmatrix} \tag{14}$$

where the entries of J have the same properties that S and the storage elements in (14) have a derivative causality. Also, D_{ind} and D_{outd} are defined by

$$D_{outd}(t) = L_d D_{ind}(t) \tag{15}$$

and they depend of the causality assignment for the storage elements and that junctions have a correct causality assignment.
From (6) to (13) and (14) we obtain,

$$z(t) = A_p^* \dot{x}(t) + B_p^* u(t) \tag{16}$$

$$y_d(t) = C_p^* \dot{x}(t) + D_p^* u(t) \tag{17}$$

where

$$A_p^* = J_{11} + J_{12} N J_{21} \tag{18}$$

$$B_p^* = J_{13} + J_{12} N J_{23} \tag{19}$$

$$C_p^* = J_{31} + J_{32} N J_{21} \tag{20}$$

$$D_p^* = J_{33} + J_{32} N J_{23} \tag{21}$$

being

$$N = \left(I_n - L_d J_{22} \right)^{-1} L_d \tag{22}$$

The state output equations of this system in integral causality are given by (6) and (7). It follows, from (1), (6), (7), (16) and (17) that,

$$A_p^* = FA_p^{-1} \tag{23}$$

$$B_p^* = -FA_p^{-1}B_p \tag{24}$$

$$C_p^* = C_p A_p^{-1} \tag{25}$$

$$D_p^* = D_p - C_p A_p^{-1} B_p \tag{26}$$

Considering $\dot{x}(t) = 0$, the steady state of a LTI MIMO system defined by

$$x_{ss} = -A_p^{-1} B_p u_{ss} \tag{27}$$

$$y_{ss} = \left(D_p - C_p A_p^{-1} B_p \right) u_{ss} \tag{28}$$

where x_{ss} and y_{ss} are the steady state of the state variables and the output, respectively.
In an approach of the BGD, the steady state is determined by

$$x_{ss} = F^{-1} B_p^* u_{ss} \tag{29}$$

$$y_{ss} = D_p^* u_{ss} \tag{30}$$

4. A bond graph model of an operational amplifier

The standard operational amplifier (op-amp) symbol is shown in Fig. 2. It has two input terminals, the inverting (-) input and the noninverting (+) input, and one output terminal. The typical op-amp operates with two Direct Current (DC) supply voltages, one positive and the other negative (Stanley, 1994).
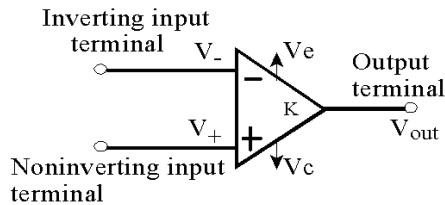

Fig. 2. Operational amplifier symbol.

The complex action of the op-amp results in the amplification of the difference between the voltages at the noninverting, V_+, and the inverting, V_-, inputs by a large gain factor, K, designed open loop gain. The output voltage is,

$$V_{out} = K \left(V_+ - V_- \right) \tag{31}$$

The assumptions of the ideal op-amp are (Barna & Porat, 1989): 1) The input impedance is infinite. 2) The output impedance is zero. 3) The open loop gain is infinite. 4) Infinite bandwidth so that any frequency signal from 0 to ∞ Hz can be amplified without attenuation. 5) Infinite slew rate so that output voltage charges simultaneously with input voltage charges.

The implications of the assumptions are: no current will flow either into or out of either input terminal of the op-amp, also, the voltage at the output terminal does not charge as the loading is varied and finally, from H_3, $V_+ - V_- = \dfrac{V_{out}}{K}$, if we take the limit when K→∞, note that $V_+ = V_-$, which indicates that the voltages at the two input terminals are forced to be equal in the limit.

The assumptions of an op-amp are not completely true in practice, and to be fully competent in the analysis and design of op-amps circuits, one must be aware of the limitations. Therefore, we propose a more realistic model applicable to DC and low frequencies based on Bond Graph with Intregral causality assignment (BGI), since an op-amp is a multistage amplifier, it can be represented by Fig. 3.
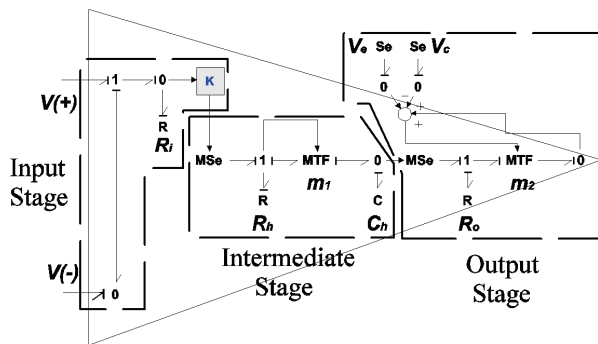

Fig. 3. Bond graph model of an operational amplifier.

The individual stages used in op-amp are separately chosen to develop different amplifier characteristics. Those amplifier characteristics which are determined by a given stage depend on whether it functions as an input stage, intermediate stage or output stage. So, the bond graph model of the op-amp is composed by 3 stages, which are:

- Characteristics of the differential input stage of an operational amplifier are the most critical factors which affect the accuracy of an op-amp in providing voltage gain. Errors effects of following stages are reduced in significance by the gain isolation provided by the first stage. This input stage considers the two input terminals of op-amp, the differential input resistance, denoted as R_i, which is the resistance between the inverting and non-inverting inputs and K is the open loop gain.
- The intermediate stage introduces the frequency compensation of the op-amp using a lag network. Also, using a MTF, the slew rate of the op-amp is considered.
- Following the input and intermediate voltage gain stages of an op-amp, it is desirable to provide impedance isolation from loads. In this way the characteristics of the gain

stages are preserved under load, and adequate signal current is made available to the load. In addition, the output stage provides isolation to the preceding stage and a low output impedance to the load. This stage is formed by the output terminal, the output resistance of the op-amp denoted as R_o and the adjustment of supply voltages, positive voltage V_c and negative voltage V_e, are applied using a MTF element.

The usefulness of the bond graph model of an operational amplifier can be shown, applying this model to $\mu A741$ op-amp by Fairchild Semiconductor Corporation (Stanley, 1994; Gayakward, 2000) and, $TL084$ and $OP27$ by Texas Instruments (Stanley, 1994; Gayakward, 2000) whose data sheets are shown in Table 1.

Op-amp	$\mu A741$	$TL084$	$OP27$
$R_i\left(\Omega\right)$	2×10^6	10^{12}	6×10^6
$R_o\left(\Omega\right)$	75	75	70
K	2×10^5	2×10^5	1.8×10^6
$SR\left(V/\mu s\right)$	0.5	13	2.8
$V_c, V_e\left(V\right)$	± 15	± 18	± 22

Table 1. Data sheets of $\mu A741$, $TL084$ and $OP27$.

Using the data sheets of an op-amp, the high cutoff frequency of the open loop voltage gain, f_o, is determined. Moreover, the compensation parameters of the bond graph model are defined by

$$f_o = \frac{1}{2\pi R_c C_c} \tag{32}$$

From (32) and the data sheets of the $\mu A741$, $TL084$ and $OP27$ op-amps, the parameters to obtain the frequency response are given in Table 2.

Op-amp	$\mu A741$	$TL084$	$OP27$
$R_h\left(\Omega\right)$	10^3	10^3	10^3
$C_h\left(F\right)$	3.06652×10^{-6}	5.3051×10^{-6}	1.9894×10^{-5}

Table 2. Parameters of frequency response.

Substituting the parameters of Tables 1 and 2 to bond graph model of each op-amp, the frequency responses of $\mu A741$, $TL084$ and $OP27$ op-amps are shown in Fig. 4, 5 and 6, respectively.

Note that, the frequency responses of the $\mu A741$, $TL084$ and $OP27$ op-amps are very close respect to the data sheets of these op-amps (Stanley, 1994; Gayakward, 2000). Also, decibel gain is $K_{dB} = 20Log\left(K\right)$. The next section an application of the bond graph model of an op-amp to prove the time response is presented.
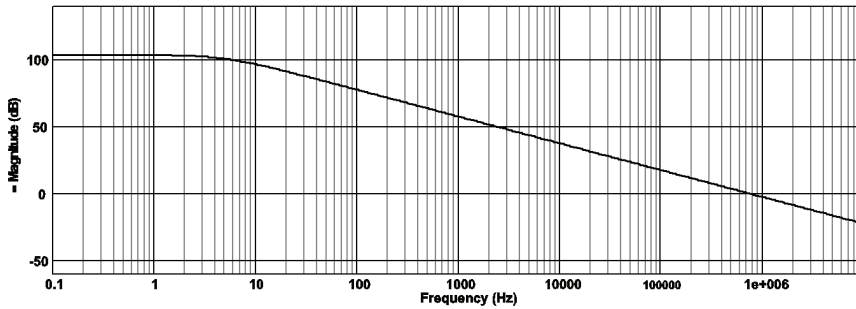
Fig. 4. Frequency response of $\mu A741$ op-amp.
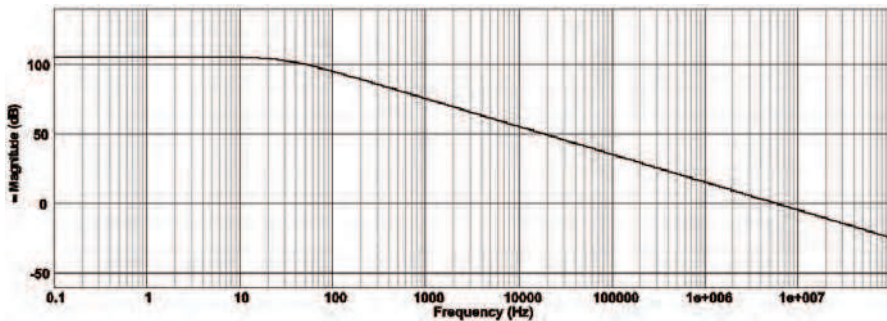

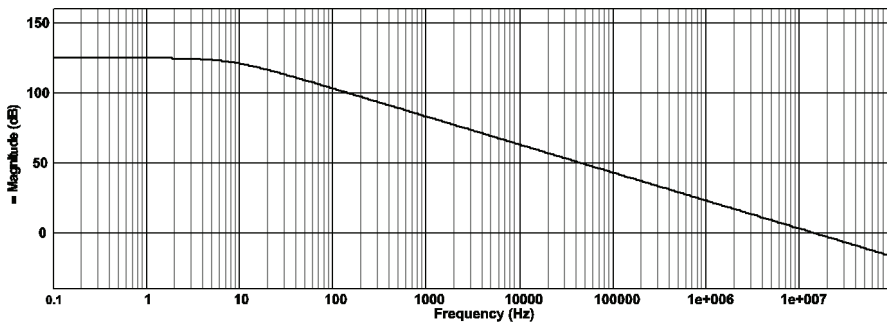Fig. 5. Frequency response of $TL084$ op-amp.

Fig. 6. Frequency response of $OP27$ op-amp.

5. Comparator circuit

Comparator circuits represent to the first class of circuits we have considered that are basically nonlinear in operation. Specifically, comparator circuits produce two or more discrete outputs, each of which is dependent on the input level (Floyd & Buchla, 1999). In this application, the op-amp is used in the open loop configuration with the input voltage on one input and a reference voltage on the other, which is shown in Fig. 7.
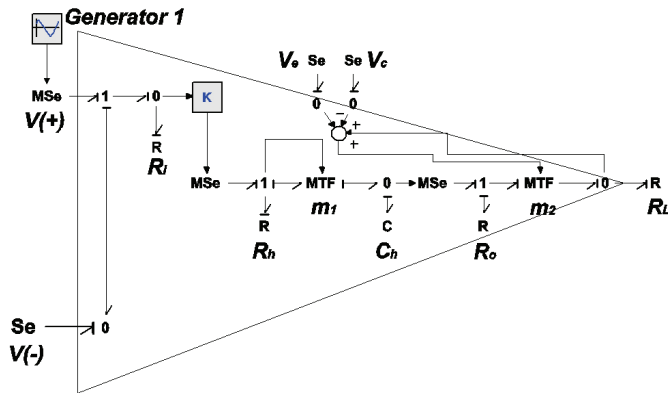
Fig. 7. Bond graph model of a comparator op-amp.

Applying a voltage $v_+(t) = 3\sin(2\pi f_+ t)V$ to the noninverting input, where $f_+ = 0.15 Hz$ and $v_- = 1V$ to the inverting input of the bond graph model of Fig. 7. Also, the supply voltages are $V_c = 12V$ and $V_e = -12V$, the time response of the comparator circuit using the $\mu A741$ op-amp is shown in Fig. 8.
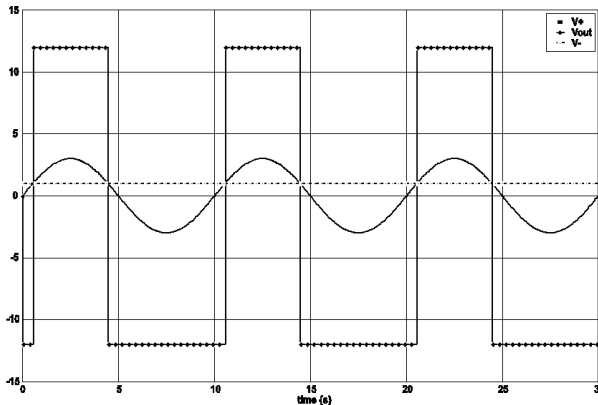

Fig. 8. Time response of the comparator op-amp.

In according with the objective of the comparator circuit, the time response of the Fig. 8 is satisfactory (Stanley, 1994; Gayakward, 2000; Floyd & Buchla, 1999). However, if the frequency of the input signal increases, we have to consider the response of phase shift versus frequency, which is obtained using the proposed bond graph model and is shown in Fig. 9 for $\mu A741$ op-amp phase shift between the input and output signals.

If the noninverting input voltage is $v_+(t) = 0.1\sin(2\pi f_+ t)V$ where $f_+ = 100 Hz$, the inverting input voltage is $v_-(t) = 0V$ and, the supply voltages are $V_c = 12V$ and

$V_e = -12V$, then the time response of the comparator circuit using $\mu A741$ op-amp is a square waveform of magnitude $\pm 12V$ and a phase shift of $\theta = -86.8^0$ respect the input signal, which is shown in Fig. 10.
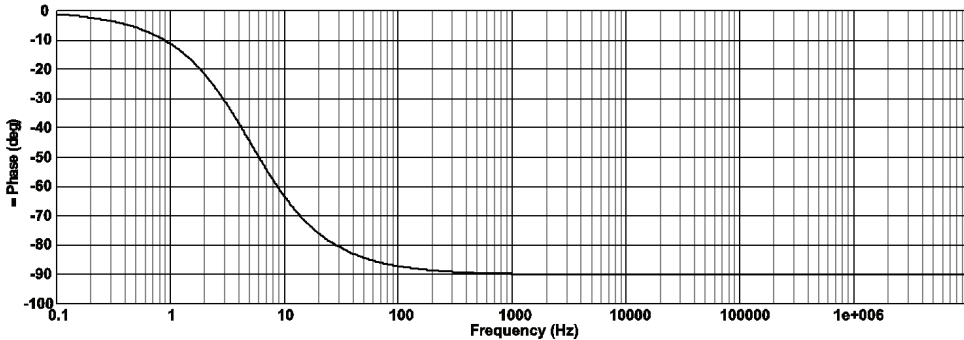

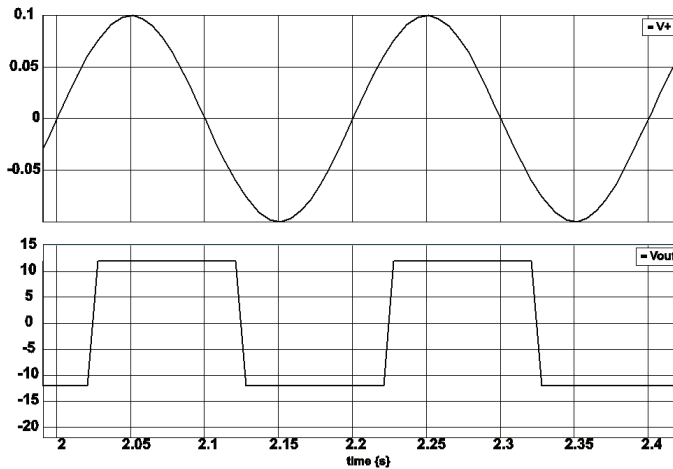Fig. 9. Phase shift versus frequency of $\mu A741$ op-amp.

Fig. 10. Time response of comparator with $V_+(t) = 20\sin(200\pi t)$.

The phase shift of the output signal of Fig. 10 can be verified from the following equation, calculating the lag time of the output signal,

$$t = \frac{\theta}{360 f} \tag{33}$$

where θ is the phase shift of the bode plot for $\mu A741$ op-amp is the Fig. 8, and f is the frequency of the input signal. In this case $t = 2.41ms$.

In next section op-amp configurations with negative feedback in the physical domain are proposed.

6. Feedback operational amplifier

An op-amp that uses feedback is called a feedback is called a feedback amplifier. A feedback amplifier is sometimes referred to as a closed loop amplifier because the feedback forms a closed loop between the input and the output. A feedback amplifier essentially consists of two parts: an op-amp and a feedback circuit. The feedback circuit can take any form whatsoever, depending on the intended application of the amplifier. This means that the feedback circuit may be made up of either passive components, active components, or combinations of both (Gayakward, 2000).

A closed loop amplifier can be represented by using two blocks, one for an op-amp and another for a feedback circuit. There are four ways to connect theses two blocks. These connections are classified according to whether the voltage or current is fed back to the input in series or in parallel, as follows: 1) Voltage series feedback, 2) Voltage shunt feedback, 3) Current series feedback and 4) Current shunt feedback (Gayakward, 2000) and (Floyd & Buchla, 1999).

The voltage series feedback configuration is one of the most important because this is commonly used. An in depth analysis of this configuration in the physical domain is presented in this section, computing voltage gain, input resistance, output resistance and the bandwidth.

6.1 A bond graph model of a noninverting amplifier

An op-amp connected in a closed loop configuration as a noninverting amplifier is shown in Fig. 11. The input signal is applied to the noninverting input. A portion of the output is applied back to the inverting input through the feedback network in the physical domain. The BGI and the Bond Graph in a Derivative causality assignment (BGD) are shown in Fig. 11, in order to get the symbolic expressions of the closed loop system in steady state applying the methodology given in section 1.
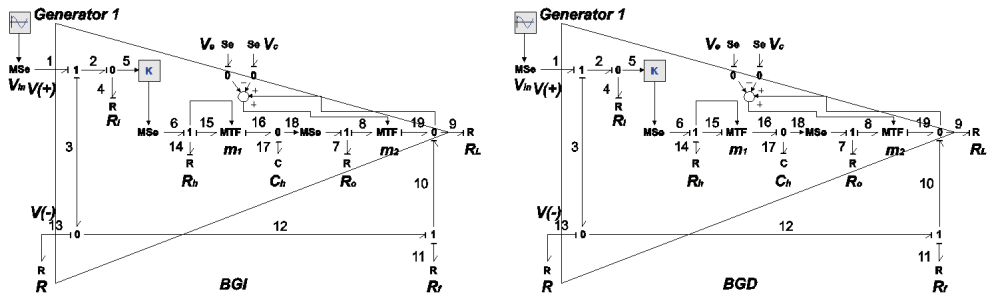

Fig. 11. Bond graph models of a noninverting amplifier.

The closed loop gain, A_{CL}, can be determined using the BGD approach, from (30) we have,

$$A_{CL} = \frac{y_{ss}}{u_{ss}} = D_p^* \qquad (34)$$

where y_{ss} and u_{ss} are the steady state values of the output and input, respectively.

We now derive the closed loop gain of the noninverting amplifier using the BGD. The key vectors of BGD are given by,

$$x(t) = q_{17}(t); \dot{x}(t) = f_{17}(t); z(t) = e_{17}(t)$$
$$u(t) = e_1(t); y(t) = e_9(t)$$
$$D_{ind}(t) = \begin{bmatrix} e_4(t) & e_7(t) & e_9(t) & f_{11}(t) & f_{13}(t) & f_{14}(t) \end{bmatrix}$$
$$D_{outd}(t) = \begin{bmatrix} f_4(t) & f_7(t) & f_9(t) & e_{11}(t) & e_{13}(t) & e_{14}(t) \end{bmatrix}$$

$$(35)$$

the constitutive relations are,

$$F = \frac{1}{C_h} \tag{36}$$

$$L_d = diag\left\{ \frac{1}{R_i}, \frac{1}{R_o}, R_F, R, R_h \right\} \tag{37}$$

and the junction structure is,

$$J_{21} = \begin{bmatrix} 0 \\ 0 \\ 0 \\ 0 \\ 0 \\ \frac{1}{m} \end{bmatrix}; J_{22} = \begin{bmatrix} 0 & 0 & 0 & 0 & -1 & 0 \\ 0 & 0 & 0 & m_2 & \frac{-K}{m_1} - m_2 & \frac{-1}{m_1} \\ 0 & 0 & 0 & -1 & 1 & 0 \\ 0 & -m & 1 & 0 & 0 & 0 \\ 1 & m_2 & -1 & 0 & 0 & 0 \\ 0 & 0 & 0 & 0 & 0 & 0 \end{bmatrix}; J_{23} = \begin{bmatrix} 1 \\ \frac{K}{m_1} \\ 0 \\ 0 \\ 0 \\ 0 \end{bmatrix}$$

$$J_{12} = \begin{bmatrix} 0 & 0 & 0 & 0 & \frac{-K}{m_1} & \frac{-1}{m_1} \end{bmatrix}; J_{32} = \begin{bmatrix} 0 & 0 & 0 & -1 & 1 & 0 \end{bmatrix} \tag{38}$$

$$J_{13} = \frac{K}{m_1}; J_{11} = J_{31} = J_{33} = 0$$

From (21), (22), (34), (36), (37) and (38), the closed loop gain of the noninverting amplifier is,

$$A_{CL} = \frac{R_L \left[m_2 R_i K \left(R + R_f \right) + m_1 R R_o \right]}{m_1 R_o \Delta + K R m_2 R_L R_i + R_L m_2^2 m_1 \left[R_f \left(R + R_i \right) + R R_i \right]} \tag{39}$$

where $\Delta = \left(R + R_i \right) \left(R_L + R_f \right) + R R_i$

Note that the closed loop gain (39) takes account the internal parameters and the external elements connected to op-amp.

A normal operation of the op-amp using the bond graph model indicates the modules of $MTF's$ are $m_1 = 1$, the slew rate is sufficient of the op-amp, and $m_2 = 1$, the supply voltages allow to obtain the output voltage depending the input voltage and the gain of the op-amp.

Considering, $m_1 = 1$, $m_2 = 1$ and $R_o = 0$, we obtain

$$\left(A_{CL} \right)_1 = \frac{R + R_f}{R + \dfrac{1}{K}\left(R_f + RR_i + \dfrac{R_f R}{R_i} \right)} \tag{40}$$

Applying the $\underset{\substack{R_i \to \infty \\ K \to \infty}}{Lim}\left(A_{CL} \right)_1$, the ideal closed loop gain of this amplifier, $\left(A_{CL} \right)_i$, is determined,

$$\left(A_{CL} \right)_i = 1 + \frac{R_f}{R} \tag{41}$$

The time response of the noninverting amplifier using $\mu A741$ op-amp, $R = 10K\Omega$, $R = 190K\Omega$ and the input signal is $v_i\left(t \right) = 0.5\sin\left(2\pi f_i t \right)V$ where $f_i = 1KHz$, is shown in Fig. 12.
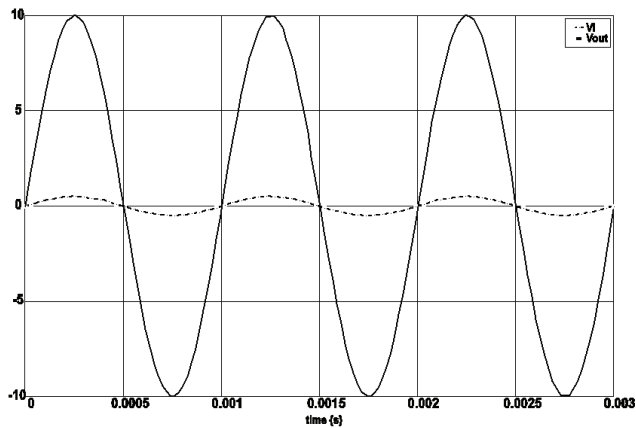

Fig. 12. Time response of the noninverting amplifier.

6.1.1 Input resistance of the noninverting amplifier

The input resistance of the noninverting amplifier can be determined using the BGD of Fig. 11. Considering the output $f_i\left(t \right)$, the submatrices J_{31}, J_{32} and J_{33} from (38) are changed by

$$J_{23} = \begin{bmatrix} 1 & 0 & 0 & 0 & 0 & 0 \end{bmatrix}; J_{13} = J_{33} = 0 \tag{42}$$

From (21), (22), (37) and (38) the input resistance is determined by,

$$R_{iF} = \frac{R_o \left[\left(R + R_i \right) \left(R_L + R_f \right) + RR_i \right] + KRR_L R_i + R_L \left[R_f \left(R + R_i \right) + RR_i \right]}{\left(R + R_f \right) \left(R_o + R_L \right) + R_o R_L} \tag{43}$$

where $\left(e_1 \right)_{ss}$ and $\left(f_1 \right)_{ss}$ are the steady state values of the input e_1 and output f_1, respectively.
If $R_o = 0$ we reduce,

$$\left(R_{iF} \right)_1 = R_i \left(1 + \frac{KR}{R + R_f} \right) + \frac{RR_f}{R + R_f} \tag{44}$$

finally, the term $\dfrac{R_f R}{R + R_f} \square R_i \dfrac{KR}{R + R_f}$ hence the ideal input resistance of the noninverting

amplifier $\left(R_{iF} \right)_i$ is defined by,

$$\left(R_{iF} \right)_i = R_i \left(1 + \frac{KR}{R + R_f} \right) \tag{45}$$

The result of (45) indicates that the ideal input resistance of the op-amp with feedback is $\left(1 + KR / R + R_f \right)$ times that without feedback. In addition, the equation (43) allows to determine the input resistance of the op-amp considering the internal parameters and external elements for this configuration. Equation (45) can be verified in (Stanley, 1994; Gayakward, 2000).

6.1.2 Output resistance of the noninverting amplifier
Output resistance is the resistance determined looking back into the feedback amplifier from the output terminal. A BGD that allows to obtain the output resistance of a noninverting amplifier is shown in Fig. 13.
The key vectors of the BGD of Fig. 13 are,

$$
\begin{aligned}
&x(t) = q_{16}(t); \dot{x}(t) = f_{16}(t); z(t) = e_{16}(t) \\
&u(t) = e_1(t); y(t) = f_1(t) \\
&D_{ind}(t) = \begin{bmatrix} e_4(t) & e_7(t) & e_{10}(t) & f_{12}(t) & e_{13}(t) \end{bmatrix} \\
&D_{outd}(t) = \begin{bmatrix} f_4(t) & f_7(t) & f_{10}(t) & e_{12}(t) & f_{13}(t) \end{bmatrix}
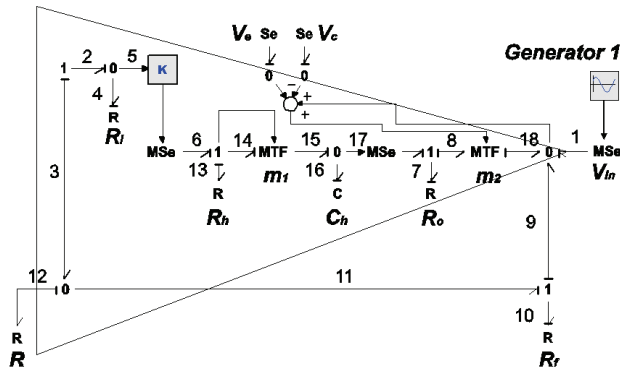\end{aligned}
\tag{46}
$$

Fig. 13. Derivation of output resistance of a bond graph model of a noninverting amplifier.

the constitutive relations are,

$$L = diag \left\{ \frac{1}{R_i}, \frac{1}{R_o}, \frac{1}{R_f}, R, \frac{1}{R_h} \right\} \tag{47}$$

$$F = \frac{1}{C_h} \tag{48}$$

and the junction structure of the BGD is,

$$J_{22} = \begin{bmatrix} 0 & 0 & 0 & -1 & 0 \\ 0 & 0 & 0 & K & -1 \\ 0 & 0 & 0 & 1 & 0 \\ 1 & 0 & -1 & 0 & 0 \\ 0 & 0 & 0 & 0 & 0 \end{bmatrix}; J_{21} = \begin{bmatrix} 0 \\ 0 \\ 0 \\ 0 \\ 1 \end{bmatrix}; J_{21} = J_{32}^T = \begin{bmatrix} 0 \\ -1 \\ -1 \\ 0 \\ 0 \end{bmatrix} \tag{49}$$

$$J_{12} = \begin{bmatrix} 0 & 0 & 0 & -K & -1 \end{bmatrix}; J_{11} = J_{13} = J_{31} = J_{33} = 0$$

Substituting (22), (47), (49) into (21) the output resistance of a noninverting amplifier is obtained,

$$R_{oF} = \frac{(e_1)_{ss}}{(f_1)_{ss}} = \left(D_p^*\right)^{-1} = \frac{R_o \left[R_i \left(R + R_f \right) + RR_f \right]}{R_i \left(R + R_f + KR \right) + RR_f + R_o \left(R + R_i \right)} \tag{50}$$

Calculating $\left(R_{oF} \right)_1 = \lim_{R_i \to \infty} R_{oF}$ we have,

$$\left(R_{oF} \right)_1 = \frac{R_o \left(R + R_f \right)}{R + R_f + KR + R_o} \tag{51}$$

finally, $R_o + R + R_f + KR \square R + R_f + KR$,   the   ideal   output   resistance $\left(R_{oF}\right)_i$ of   the noninverting amplifier is given by,

$$\left(R_{oF}\right)_i = \frac{R_o}{1 + \dfrac{KR}{R + R_f}}$$

(52)

This result shows that the ideal output resistance of the noninverting amplifier is $\dfrac{1}{\left(1 + KR/R + R_f\right)}$ times the output resistance R_o of the op-amp. That is , the output resistance of the op-amp with feedback is much smaller than the output resistance without feedback. In addition (52) can be verified in (Stanley, 1994; Gayakward, 2000).

6.1.3 Bandwidth of the noninverting amplifier
The bandwidth of an amplifier is defined as the band (range) of frequency for which the gain remains constant. Manufacturers generally specify either the gain-bandwidth product or supply open loop gain versus frequency curve for the op-amp (Gayakward, 2000).
Fig. 4 shows the open loop gain versus frequency curve of the $\mu A741$ op-amp. From this curve for a gain of 200,000, the bandwidth is approximately $5Hz$; or the gain-bandwidth product is $1MHz$. On the other extreme, the bandwidth is approximately $1MHz$ when the gain is 1. Hence, the frequency at which the gain equals 1 is known as the unity gain bandwidth (UGB).

Since for an op-amp with a single break frequency f_o , the gain-bandwidth product is constant, and equal to UGB, we can write,

$$UGB = \left(K\right)\left(f_o\right) = \left(A_{CL}\right)\left(f_F\right)$$

(53)

where f_F bandwidth with feedback.

Therefore, the bandwidth of an feedback op-amp is,
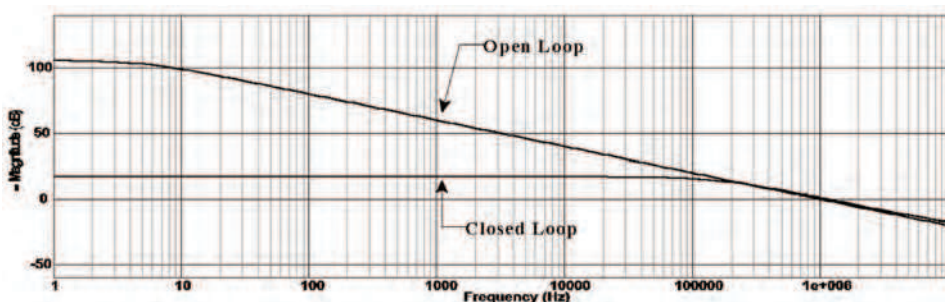
$$f_F = \frac{(K)(f_o)}{A_{CL}}$$

(54)

Fig. 14. Frequency response of the noninverting amplifier.

The frequency response of the noninverting amplifier based on BGI of Fig. 11, using $\mu A741$ op-amp, $R = 1K\Omega$, $R_f = 5K\Omega$ and the input signal is $v_i(t) = 1.0\sin(2\pi f_i t)V$ where $f_i = 30KHz$, is shown in Fig. 14.

Note that the frequency response of this amplifier indicates that the closed loop gain is $A_{CL} = 6 = 15.56dB$ until approximately $166KHz$, which is verified from (54).

6.1.4 Slew rate

Another important frequency related parameter of an op-amp is the slew rate. The slew rate is the maximum rate of change of output voltage with respect to time, usually specified in $V/\mu s$. Ideally, we would like an infinity slew rate so that the op-amp's output voltage would change simultaneously with the input. Practical op-amps are available with slew rates from $0.1V/\mu s$ to well above $1000V/\mu s$. The slew rate (SR) can be obtained by,

$$SR = \frac{2\pi f V_p}{10^6} V / \mu s \qquad (55)$$

where f is the input frequency and V_p is the peak value of the output sine wave.

In order to show the effect of the slew rate of an op-amp, the time responses of the noninverting amplifier based on BGI of Fig. 11, using $\mu A741$ and $OP27$ op-amps, $R = 1K\Omega$, $R_f = 5K\Omega$ and the input signal is $v_i(t) = 1.0\sin(2\pi f_i t)V$ where $f_i = 30KHz$, are shown in Fig. 15. The ideal closed gain is then $(A_{CL})_i = 6$.
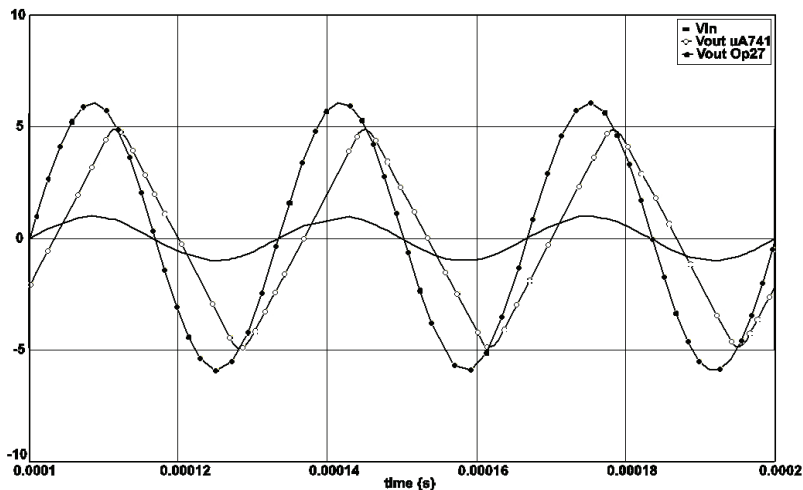

Fig.15. Effect of the slew rate of the noninverting amplifier using $\mu A741$ and $OP27$ op-amps.

Thank You for previewing this eBook

You can read the full version of this eBook in different formats:

- ➢ HTML (Free /Available to everyone)

- ➢ PDF / TXT (Available to V.I.P. members. Free Standard members can access up to 5 PDF/TXT eBooks per month each month)

- ➢ Epub & Mobipocket (Exclusive to V.I.P. members)

To download this full book, simply select the format you desire below